MECHANOCHEMISTRY AND MECHANICAL ALLOYING 2003

JOURNAL OF MATERIALS SCIENCE **39** (2004) 5143– 5146

Mechanochemical synthesis of nanoparticles

TAKUYA TSUZUKI*, PAUL G. McCORMICK
Research Centre for Advanced Mineral and Materials Processing, University of Western Australia, 35 Stirling Highway, Crawley, WA 6009, Australia
E-mail: takuya@mech.uwa.edu.au

The results of recent investigation of the mechanochemical synthesis of inorganic nanoparticles are reviewed. It was demonstrated that, by selecting suitable chemical reaction paths, stoichiometry of starting materials and milling conditions, mechanochemical processing can be used to synthesise a wide range of nanocrystalline particles dispersed within a soluble salt matrix. Selective removal of the matrix phase by washing the resulting powder with appropriate solvents can yield nanoparticles of the desired phase. This technique has been shown to have advantages over other methods of producing nanoparticles in terms of low cost, small particle sizes, low agglomeration, narrow size distributions and uniformity of crystal structure and morphology.

1. Introduction

Nano-size particles of less than 100 nm in diameter are currently attracting increasing attention for the wide range of new applications in various fields of industry [1]. Such powders can exhibit properties that differ substantially from those of bulk materials, as a result of small particle dimension, high surface area, quantum confinement, and other effects. Most of the unique properties of nanoparticles require not only the particles to be of nano-sized, but also the particles be dispersed without agglomeration.

Many methods have been developed for the synthesis of nanoparticles, including vapour phase condensation, sputtering, wet chemical precipitation, sol-gel techniques and hydrothermal synthesis. Since many existing methods involve the nucleation of nanoparticles in either vacuum, gas or liquid, the separation of nanoparticles during synthesis is not guaranteed: Particles encounter one after another in the growth stage, resulting in the formation of agglomeration and relatively poor control of the overall particle size distribution.

The synthesis of nanocrystalline materials by mechanical milling, mechanical alloying [2] and mechanochemical processing [3] has been widely studied. Those milling techniques enable synthesis of nanocrystalline structures in the as-milled powder, due to the process of particle deformation and fracture that accompanies repeated ball-powder collision events. Recently, it has been demonstrated that mechanochemically induced solid-state reactions can also be used for the production of nanoparticles.

This paper reviews recent research concerned with the synthesis of nanoparticles by mechanochemical processing carried out at the Research Center for Advanced Mineral and Materials Processing.

2. Nanoparticle synthesis by mechanochemical processing

Mechanochemical processing is characterised by the repeated welding, deformation and fracture of the mixture of reactants. Chemical reactions occur at the interfaces of the nanometer-sized grains that are continuously re-generated during milling [4]. As a consequence, chemical reactions, which would normally require high temperatures to occur due to separation of the reacting phases by the product phases, can occur at low temperatures in a ball mill without any need for external heating [5]. The reactions may occur either in a steady-state manner or self-propagating combustive manner [6, 7]. Solid-state displacement reactions that occur in a combustive manner lead to micron-sized particles due to high temperature, whilst the reactions that occur in a steady state manner result in a nanoscale mixture of product phases [8]. Mechanochemical combustion can be avoided by appropriate selection of milling parameters to reduce collision energy and by addition of inert diluents to the starting powder mixture to reduce the reaction rate.

By selecting suitable conditions such as chemical reaction paths, stoichiometry of starting materials and milling conditions, mechanochemical processing can be used to synthesise nanocrystalline particles dispersed within a soluble salt matrix. Selective removal of the matrix phase by washing the resulting powder with appropriate solvents can yield nanoparticles of the desired phase as small as 5 nm [9].

Of significance is the fact that this technique allows the formation of separated nanoparticles embedded in a solid matrix, leading to agglomeration–free nanopowders. Moreover, the crystallinity of nanoparticles can be improved by heat treatment prior to removal of the

---

*Author to whom all correspondence should be addressed.

TABLE I Examples of mechanochemical reactions and associated enthalpy change ΔH

	Reaction	ΔH (kJ/mole)
(1)	$FeCl_3 + 3\ Na \rightarrow Fe + 3\ NaCl$	−884
(2)	$CoCl_2 + 2\ Na \rightarrow Co + 2\ NaCl$	−495
(3)	$NiCl_2 + 2\ Na \rightarrow Ni + 2\ NaCl$	−507
(4)	$CuCl_2 + 2\ Na \rightarrow Cu + 2\ NaCl$	−575

solid matrix phase without inducing particle agglomeration due to the enclosure of nanoparticles in the solid matrix.

3. Metal nanoparticles

Studies to date have demonstrated the mechanochemical synthesis of ultrafine Fe, Co, Ni, Cu, Ag, Ta, and W powders [10–13]. A list of selected mechanochemical reactions is given in Table I.

The reactions in Table I were all highly exothermic, and hence the use of diluent was necessary to avoid combustion. In the studies carried out using Spex 8000 mixer/mill, the collision energy was reduced by decreasing the diameter of grinding media. It was shown that the decreasing the grinding ball size from 12.6 mm to 3.2 mm delayed the onset of combustion during the milling of $CuCl_2 + 2$ Na starting mixture [10]. However, in order to prevent combustion from occurring, it was necessary to add 100 wt% NaCl as a diluent phase into the starting mixture. Other reactions in Table I also required addition of NaCl for the prevention of combustion.

Fig. 1 shows a nickel-mapping transmission electron micrograph of an as-milled particle after milling for 2 h to cause the reaction (3) in Table I [13]. It is evident that, although the particle size of Ni/NaCl nanocomposite was ∼500 nm, it consisted of ∼5 nm sized Ni nanoparticles embedded and dispersed within a solid matrix of NaCl. After washing the powder with deionised deoxygenated water, Ni nanoparticles were obtained as shown in the transmission electron microscopy (TEM) image (Fig. 2).

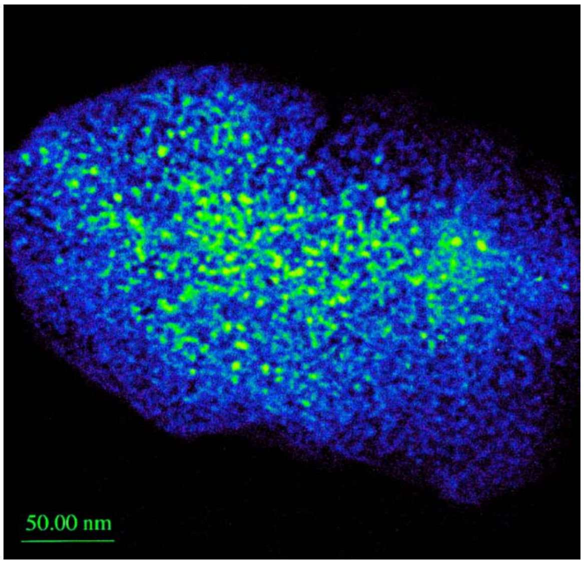

Figure 1 Nickel mapping TEM image of an as-milled particle [13].

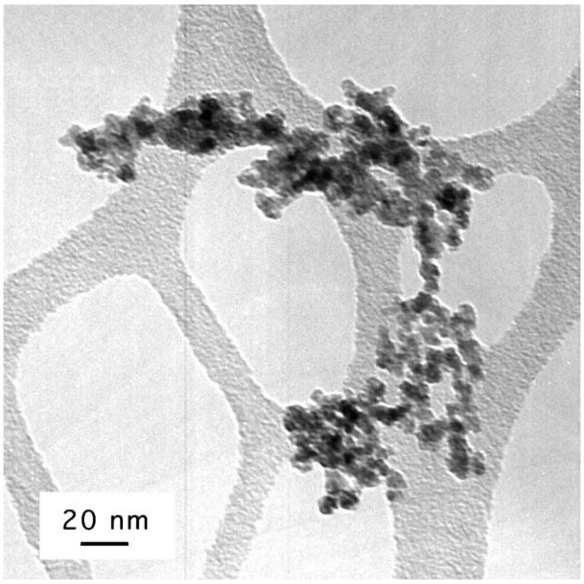

Figure 2 TEM image of Ni nanoparticles [13].

Milling for longer time resulted in the particle growth due to inter-particle welding during collision events. On the other hand, milling of micron-sized Ni and NaCl powders, i.e., top-down approach to grind down Ni particles, resulted in a layered particle morphology, and the particle size was ∼10 μm even after milling for 16 h [13].

4. Oxide nanoparticles

Various oxide nanoparticles have been synthesised by mechanochemical processing, including Al_2O_3 [14], ZrO_2 [15, 18], Gd_2O_3 [16], CeO_2 [17], Cr_2O_3 [19], Nb_2O_5 [20], SnO_2 [21, 22], Fe_2O_3 [23] and ZnO [24]. A list of mechanochemical reactions used for the synthesis of oxide nanoparticles is given in Table II.

It was found that the volume fraction of nanoparticles in the product phase should be sufficiently low to prevent the crystallite of the desired phase from being interconnected or percolated through the composite as-milled particles. For example, SnO_2 nanoparticles were produced via the reaction $SnCl_2 + Ca(OH)_2 + 0.5\ O_2 \rightarrow SnO_2 + CaCl_2 + H_2O$ and subsequent heat treatment, but the resulting powder comprised large (∼400 nm) aggregates. When $CaCl_2$ diluent was added in the starting powder mixture to decrease

TABLE II Examples of mechanochemical reactions

Reaction
$2AlCl_3 + CaO \rightarrow Al_2O_3 + 3CaCl_2$
$ZrCl_4 + 2CaO \rightarrow ZrO_2 + 2CaCl_2$
$GdCl_3 + 3NaOH \rightarrow Gd_2O_3 + 3NaCl + 1.5H_2O$
$CeCl_3 + NaOH \rightarrow CeO_2 + 3NaCl + H_2O$
$Na_2Cr_2O_7 + S \rightarrow Cr_2O_3 + Na_2SO_4$
$2NbCl_5 + 5Na_2CO_3 \rightarrow Nb_2O_5 + 10NaCl + 5CO_2$
$SnCl_2 + Na_2CO_3 + O_2 \rightarrow SnO_2 + 2NaCl + CO_2$
$2FeCl_3 + 3Ca(OH)_2 \rightarrow Fe_2O_3 + 3CaCl_2 + 3H_2O$
$ZnCl_2 + Na_2CO_3 \rightarrow ZnO + 2NaCl + CO_2$

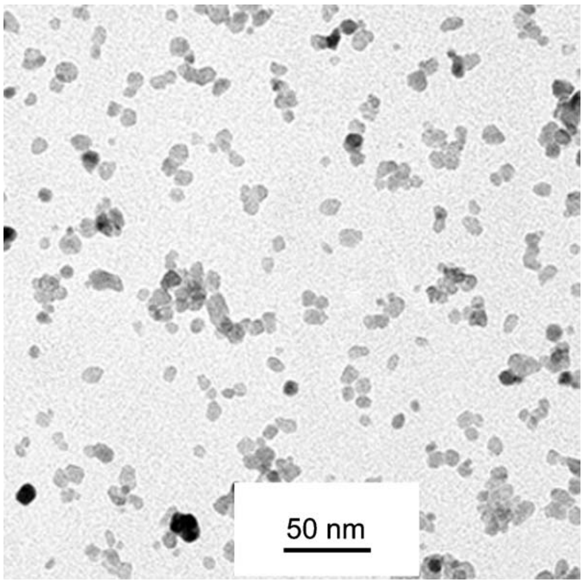

Figure 3 TEM image of CeO_2 nanoparticles [9].

the volume fraction of SnO_2 from 29 to 9%, nanoparticles of ∼40 nm in diameter were obtained [22].

CeO_2 nanoparticles of ∼10 nm were produced via the reaction $CeCl_3 + 3NaOH + 12NaCl \rightarrow Ce(OH)_3 + 15NaCl$ and subsequent heat treatment at 500°C [17]. Fig. 3 shows the CeO_2 nanoparticles thus obtained. The Brunauer-Emmett-Teller (BET) specific surface area was 83 m^2/g, corresponding to a spherical particle size of 10 nm. The crystallite size estimated from the peak broadening of an X-ray diffraction (XRD) pattern was 10.2 nm. The agreement between TEM, BET and XRD sizes is indicative of significantly low degree of agglomeration in the nanopowder.

The CeO_2 nanoparticles showed particle growth as the heat treatment temperature increased. Above the melting point of the NaCl matrix, 800°C, the particle size showed drastic increase. At the same time, the sizes estimated by BET and static laser-light scattering (LLS) spectroscopy became significantly larger than the XRD crystallite size (Fig. 4). This is due to the fact that the NaCl matrix phase was no longer solid and hence nanoparticles were not separated from each other [17].

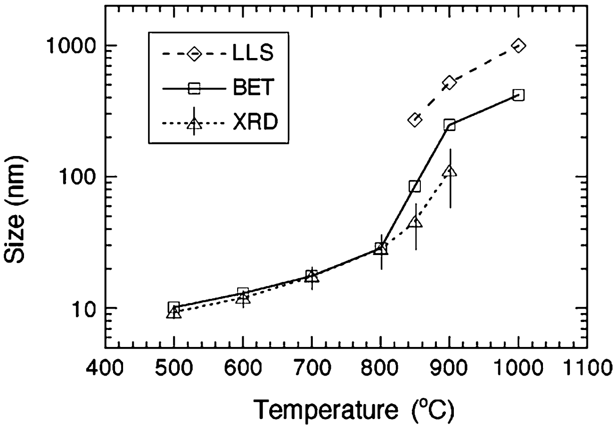

Figure 4 Particle sizes of CeO_2 nanoparticles as a function of heat treatment temperature [17].

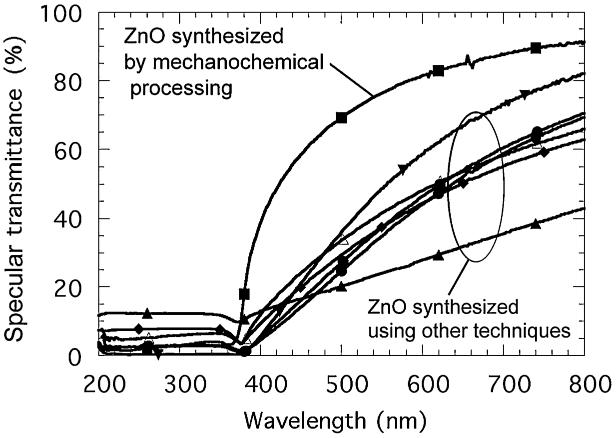

Figure 5 UV-Vis spectra of ZnO nanoparticle aqueous suspension (0.01 wt%, 10 mm optical path length).

When the particle diameter is less than one tenth of the wavelength of probe light, the light-scattering power of a particle is proportional to the 6th power of its diameter. Hence, optical extinction, i.e., light transmittance or turbidity of nanoparticle suspensions is highly sensitive to mean particle size, size distribution and agglomeration-states of nanoparticles. As shown in Fig. 5, ZnO nanoparticles synthesised by mechanochemical processing had significantly higher specular transmittance than the ZnO nanoparticles produced other methods such as physical vapour synthesis and hydrothermal synthesis [25], indicative of superiority of mechanochemical processing over other techniques.

5. Sulphide nanoparticles

Nanoparticles of ZnS, CdS and Ce_2S_3 have been synthesised by mechanochemical processing [26]. It was shown that mean particle size of ZnS nanoparticles was reduced when (i) the particle-size of a starting reactant was reduced, (ii) the size of milling media was reduced, or (iii) the volume fraction of ZnS in the product phase was reduced [27].

CdS nanoparticles were synthesised using the reaction $Na_2S + CdCl_2 + 15.6\ NaCl \rightarrow CdS + 17.6\ NaCl$ [28]. It was possible to control mean particle sizes from 4 to 8 nm by varying the size of grinding media. After milling for 4 hours with milling media of 4.8 mm in diameter and subsequent washing to remove NaCl, CdS nanoparticles of ∼4 nm in diameter were obtained. Crystallite size determined from X-ray diffraction study was 4.3 nm. As shown in Fig. 6, TEM study showed that the particles had a narrow size distribution.

CdS is a II–VI semiconductor with a direct bandgap of 2.4 eV. Quantum size effects are expected for particles smaller than the exciton Bohr diameter of 8 nm. The CdS synthesised by mechanochemical processing showed a blue-shift of the absorption energy, indicative of a quantum size effect [28, 29].

6. Carbonate nanoparticles

$CaCO_3$ nanoparticles were obtained via the reaction of $CaCl_2 + Na_2CO_3 + 10.3\ NaCl \rightarrow CaCO_3 + 12.3$

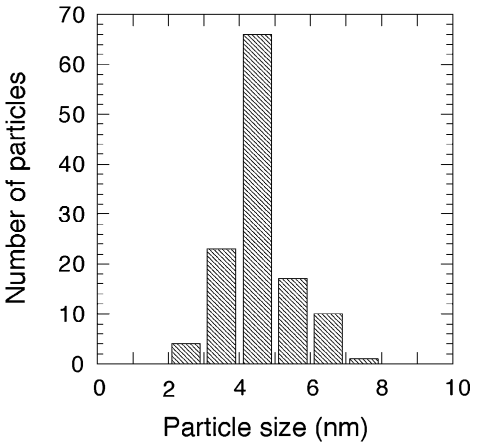

Figure 6 Size distribution of CdS nanoparticles by TEM study.

NaCl [30]. The powder consisted of 10–80 nm size nanoparticles having a calcite structure and a cuboidal morphology. Commercial production of ultrafine $CaCO_3$ uses a wet chemical precipitation technique, which is difficult to create a homogeneous reaction environment in a large scale reactor, leading to agglomerated particles having a wide variety of crystal structures and morphologies [31]. In contrast, mechanochemical processing enables building up nanoparticles through solid-state chemical reactions in a nano-scopically uniform environment, and thus the resulting nanoparticles normally have uniform structure and morphology and a narrow size distribution.

7. Summary

A wide range of nanoparticles have been synthesised by mechanochemical processing. The process involves mechanochemically activated solid-state reactions and subsequent removal of matrix phases. In order to produce small particle sizes, it was necessary to (i) avoid combustion during milling, (ii) reduce volume fraction of the particle phase, (iii) carefully control milling conditions such as grinding-media size and milling time. The resulting nanoparticles have mean particle sizes as small as 4 nm, low agglomeration, narrow size distributions and uniformity of crystal structure and morphology, which are unique features of mechanochemically synthesised nanoparticles and are superior to the nanoparticles produced by other techniques.

References

1. M. C. ROCO, *J. Nanoparticle Res.* **1** (1999) 1.
2. P. G. McCORMICK, *Mater. Trans. JIM* **36** (1995) 161.
3. G.B. SHAFFER and P. G. McCORMICK, *Appl. Phys. Lett.* **55** (1989) 45.
4. C. C. KOCH, *Mater. Sci. Technol.* **15** (1991) 193.
5. H. YANG and P. G. McCORMICK, *Metall. Mater. Trans.* B **29** (1998) 449.
6. L. TAKACS, *Appl. Phys. Lett.* **69** (1996) 436.
7. G. B. SHAFFER and P. G. McCORMICK, *J. Mater. Sci. Lett.* **9** (1990) 1014.
8. J. DING, W. F. MIAO, P. G. McCORMICK and R. STREET, *Appl. Phys. Lett.* **69** (1995) 3804.
9. P. G. McCORMICK, T. TSUZUKI, J. S. ROBINSON and J. DING, *Adv. Mater.* **13** (2001) 1008.
10. J. DING, T. TSUZUKI, P. G. McCORMICK and R. STREET, *J. Alloys and Compd.* **234** (1996) L1.
11. *Idem.*, *J. Phys. D: Appl. Phys.* **29** (1996) 2365.
12. *Idem.*, *J. Magn. Magn. Mater.* **162** (1996) 2956.
13. *Idem.*, *J. Mater. Sci.* **34** (1999) 5293.
14. *Idem.*, *J. Amer. Ceram. Soc.* **79** (1996) 2956.
15. *Idem.*, *Nanostr. Mater.* **8** (1997) 75.
16. T. TSUZUKI, E. PIRAULT and P. G. McCORMICK, *ibid.* **11** (1999) 125.
17. T. TSUZUKI and P. G. McCORMICK, *J. Amer. Ceram. Soc.* **84** (2001) 1453.
18. A. C. DODD, T. TSUZUKI and P. G. McCORMICK, *Mater. Sci. Eng.* A **301** (2001) 54.
19. T. TSUZUKI and P. G. McCORMICK, *Acta Mater.* **48** (2000) 2795.
20. *Idem.*, *Mater. Trans.* **42** (2001) 1623.
21. L. M. CUKROV, T, TSUZUKI and P. G. McCORMICK, *Scripta Mater.* **44** (2001) 1787.
22. T. TSUZUKI and P. G. McCORMICK, *Mater. Sci. Forum* **343–346** (2000) 383.
23. J. DING, T. TSUZUKI and P. G. McCORMICK, *Nanostr. Mater.* **8** (1997) 739.
24. T. TSUZUKI and P. G. McCORMICK, *Scripta Mater.* **44** (2001) 1731.
25. T. TSUZUKI, J. S. ROBINSON and P. G. McCORMICK, *J. Aust. Ceram. Soc.* **38** (2002) 15.
26. T. TSUZUKI and P. G. McCORMICK, *Nanostr. Mater.* **12** (1999) 75.
27. T. TSUZUKI, J. DING and P. G. McCORMICK, *Physica* B **239** (1997) 378.
28. T. TSUZUKI and P. G. McCORMICK, *Appl. Phys.* A **65** (1997) 607.
29. P. N. H. NAKASHIMA, T. TSUZUKI and P. G. McCORMICK, *J. Appl. Phys.* **85** (1999) 1556.
30. T. TSUZUKI, K. PETHICK and P. G. McCORMICK, *J. Nanoparticle Res.* **2** (2000) 375.
31. J. A. WOJCIK and A. G. JONES, *Chem. Eng. Sci.* **53** (1998) 1097.

Received 11 September 2003
and accepted 27 February 2004